Design of Resonance Damping via Control Synthesis

Richard Y. Zhang, Al-Thaddeus Avestruz, Jacob K. White, and Steven B. Leeb
Department of Electrical Engineering & Computer Science
Massachusetts Institute of Technology
Cambridge, MA 02139, USA
{ryz, avestruz, white, sbleeb}@mit.edu

***Abstract*—Dampers are widely used in power electronics to damp resonances, in order to reduce device stress, power loss, and electromagnetic interference. In this paper we formulate the damping problem so as to expose the fundamental trade-off between damping amplitude peaks and minimizing power dissipation, and then use a constrained optimization approach to compute optimal Pareto frontier as a function of damper order. We use the procedure to demonstrate the diminishing returns of increasing damper order using a simple filter example, and then we demonstrate the power of the method for multiport converters. In particular, we show that using the constrained optimization procedure dramatically outperforms the standard port-by-port method.**

I. Introduction

Dampers are important in power electronics because not all spurious resonances can be absorbed into or eliminated in a design. The consequence of damping is power dissipation, but striking a balance becomes difficult in circuits of increasing complexity. This paper presents a computational approach to damper design. Section II outlines the typical considerations in damper design, and these are reformulated into a control synthesis problem in Section III, by interpreting the damper as a passive controller, and the resonance damping and dissipation considerations as the $\mathcal{H}_\infty$ and $\mathcal{H}_2$ norms of certain closed-loop plants. The reformulation is exact, meaning that the globally optimal solution to the control synthesis problem also produces the globally optimal damper design.

In Section IV, we provide a design example for a high-order damper. The computational approach is used to produce the trade-off frontier for each damper order, and the corresponding improvement in the frontier is quantified. In Section V, a complementary example is provided for the damping of a high-order plant with numerous coupled resonances. The computation approach is used to design 10 dampers simultaneously, while respecting all coupled resonances. This produced a design that dissipated 63% less power than one obtained by designing each damper individually.

II. Damper Design Considerations

The damper design problem begins with a power electronics circuit, driven by an external input, as illustrated in Fig. 1. By virtue of being low-loss, the circuit is prone to suffer from poorly damped resonances, either by design or as parasitics.

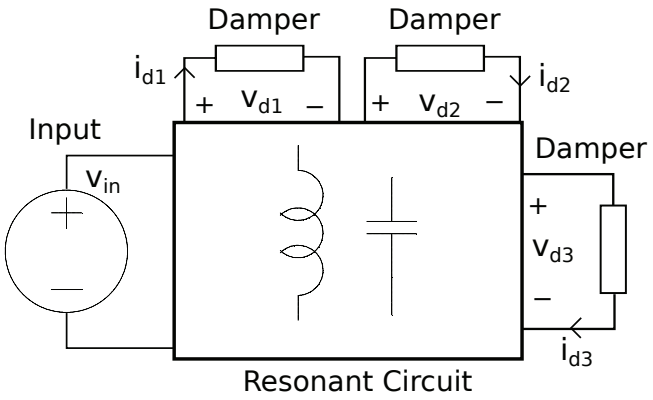

Figure 1: Damper design block diagram with 3 damper terminals

If left unmitigated, the resonances can build up to damaging voltage levels, as well as causing electromagnetic interference.

To prevent this, damper circuits are commonly placed into the circuit across those terminals identified to experience significant voltage resonance. The design of the damper circuits is an exercise in balancing competing objectives. A well-designed damper should introduce sufficient energy dissipation to dampen internal resonances on its own, but no more than necessary, because dissipation also worsens the efficiency of the overall circuit.

In power electronics, the usual practice is to choose the least-dissipative damper that still guarantees a particular *maximum frequency response*. This design rule may be phrased as an optimization,

$$\begin{array}{ll} \text{minimize} & \text{total dissipation} \\ \text{subject to} & \text{max freq response} \leq \text{specs.} \end{array} \tag{1}$$

The remainder of this section reviews each design consideration and outlines the underlying mathematical formalism.

A. Maximum frequency response

Physically, the maximum frequency response is defined to be the maximum sinusoidal peak seen at the damper terminals, due to a sinusoid of unit peak and arbitrary frequency placed

978-1-4673-6847-6/15/$31.00 ©2015 IEEE

at the inputs of the circuit. In simpler words, it represents the worst sustained resonance as seen at the damper terminals.

Mathematically, let the input-output relationship between the input and the damper terminals be described by the transfer function $T(s)$, as in

$$v_s(s) = T(s)v_{in}(s).$$

Then the maximum frequency response, written T_{max}, is the maximum modulus of $T(s)$ over all frequencies,

$$T_{max} \triangleq \max_{\omega\in\mathbb{R}} |T(j\omega)|. \tag{2}$$

In fact, it is possible to show that T_{max} coincides with the maximum root-mean-square (RMS) voltage seen at the damper terminals, due to an *arbitrary waveform* of unit RMS voltage at the input [1, Ch. 4.5].

The maximum frequency response is broadly pertinent in power electronics because it is related to how electromagnetic compatibility (EMC) regulations are specified. EMI limits are specified as spectral masks in the frequency domain; they specify the peak conducted or radiated power within a resolution bandwidth. In practice, this might mean measuring the EMI spectrum in the prescribed way and then designing a weighting filter at the plant outputs to enforce the regulatory peak spectral limits [2].

The maximum frequency response is also widely used in the design of snubbers, i.e. circuits used to protect voltage-sensitive devices from damaging voltage spikes. In this sense, the maximum RMS voltage is used as a proxy for the maximum *instantaneous* voltage. In the case of simple, low-order systems, such as the classic LC or LCL output filters, the approach is justified by the fact that the two quantities are closely related [3, p.118]. This is not necessarily the case for high-order systems, for which waveforms may be impulse-like, thereby yielding low RMS values but very high instantaneous peaks. In these cases, a nonlinear voltage clamp may be added to guarantee an instantaneous voltage threshold. The clamp can be sized to be very small, because it would activate only during those seldom occasions when the instantaneous value greatly exceeds the RMS.

B. Worst-case dissipation

Given all dampers that achieve a specified maximum frequency response, our objective is to select the one with the least dissipation. But the intuition needs to be made precise. The exact value of dissipation, and hence, the corresponding "optimal" damper, are both dependent on the *input voltage waveform*. For example, the damper that minimizes dissipation due to a sinusoid at the system resonant frequency will likely be different to the one that minimizes the dissipation due to a PWM waveform of a certain switching frequency. Indeed, it may indeed be the case that an optimal damper for one is unacceptably suboptimal for another.

Instead, a more robust approach is to design the damper to minimize worst-case dissipation over an *entire class* of input waveforms, representative of those encountered in practice. In turn, the actual value of the worst-case dissipation serves as an upper bound for the dissipation under regular conditions. Since the damper components must be sized to withstand the worst-case anyway, the approach is a practically significant for damper design.

Given a fixed class of input waveforms, $\mathcal{U}$, the worst-case dissipation is defined as the solution of the optimization problem

$$P_{max} = \begin{array}{ll} \max & \int_{-\infty}^{\infty} v_d(t)i_d(t)\,\mathrm{d}t, \\ \text{subject to} & v_{in}(t) \in \mathcal{U}, \end{array} \tag{3}$$

in which we have written $v_d(t)$ and $i_d(t)$ as the damper voltage and current waveforms due to the input voltage waveform $v_{in}(t)$.

In this paper, we consider the class of *zero-mean* input waveforms, generated by a *switching process of unit increment*, with switching frequency up to ω_{sw}, which we denote $\mathcal{BV}(\omega_{sw})$. The seemingly abstract description in fact encompasses a wide variety of practical power electronic waveforms, including:

- Two-level and multi-level converter waveforms generated by a PWM process of switching frequency up to ω_{sw}, such as those arising in [4], [5];
- Stair-case approximations of arbitrary waveforms, with quantization frequency up to ω_{sw}, like those in [6], [4];
- Resonant and quasi-resonant waveforms, with switching frequencies up to ω_{sw}, as in [7].

The advantage of $\mathcal{BV}(\omega_{sw})$ is that it be entirely defined via its spectral content due to the following elementary result from harmonic analysis.

Proposition 1 ([8, p. 23])**.** *Let f be a periodic function with bounded variation Λ. Then the n-th Fourier coefficient of f, denoted $\hat{f}_n$, is bounded from above,*

$$\hat{f}_n \leq \frac{\Lambda}{2\pi|n|}. \tag{4}$$

The definition in (4) is precise but difficult to work with. Instead we make an approximation

$$\mathcal{U} = \left\{ v(t) : |\hat{v}(j\omega)| \leq \left| \frac{\omega_{sw}}{j\omega + \omega_{sw}} \right| \right\}, \tag{5}$$

to result in an easier optimization problem in Section III. Effectively, the set $\mathcal{U}$ contains all waveforms whose Fourier spectrum is bound from above by the transfer function of a single pole placed at $\omega = 1$.

To illustrate the fact that $\mathcal{U}$ does indeed approximate $\mathcal{BV}(\omega_{sw})$, consider the spectrum of a severely aliased two-level PWM waveform in Fig. 2. Despite the seemingly random modulation and severe distortion of the output, the output spectrum is entirely encompassed within the $1/(j\omega + 1)$ envelope.

III. Control Synthesis Formulation

The damper design problem as posed in (1) is well-defined but difficult to solve. The reason lies in the need to enforce constraints with infinite dimensionality. The maximum frequency response in (2) is obtained by exhaustively examining

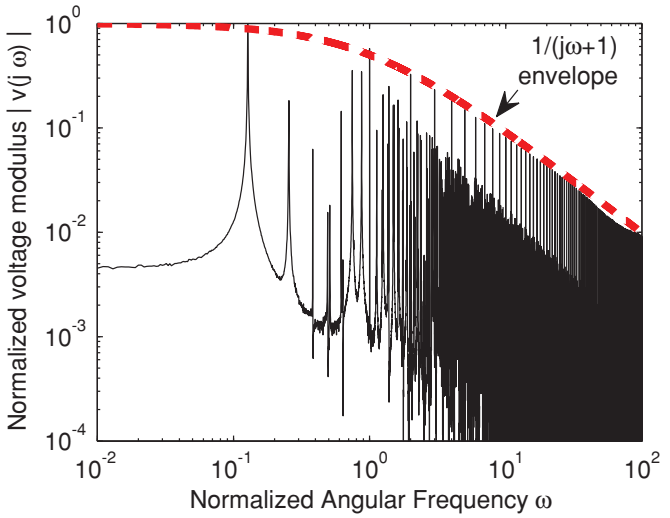

Figure 2: Spectrum of a unit-magnitude PWM waveform with switching frequency at $\omega = 1$ rad/s enclosed within an envelope of a single pole placed at $\omega = 1$.

all frequencies, and the worst-case dissipation in (3) by exhaustively examining all input waveforms of a particular class.

Instead, this section describes the steps that reformulates damper design into a control synthesis problem, in which the damper is interpreted as a fixed-order controller, and the objective P_{max} and constraint T_{max} are expressed in terms of the $\mathcal{H}_2$ and $\mathcal{H}_\infty$ norms of certain closed-loop plants. The formulation is exact, meaning that a globally optimal solution to a specific instance of the controller synthesis problem is equivalently a globally optimal damper for the corresponding damper design problem.

A. State-space models

The controller synthesis formulation begins by formulating state-space models for the input-output relationship between the damper terminal voltage, the external input voltage, and the damper current injection, and also for the admittance of the damper, as in

$$v_d(s) = T_{d,in}(s)v_{in}(s) + T_{d,d}(s)i_d(s), \tag{6}$$
$$i_d(s) = Y(s)v_d(s), \tag{7}$$

in which each transfer function is defined

$$T_{d,in}(s) = D_{d,in} + C_d(sI - A)^{-1}B_{in}, \tag{8}$$
$$T_{d,d}(s) = D_{d,d} + C_d(sI - A)^{-1}B_d, \tag{9}$$
$$Y(s) = D_Y + C_Y(sI - A_Y)^{-1}B_Y. \tag{10}$$

Given physical circuit schematics, the data matrices $A, B_{in}, B_d, C_d, D_{d,in}, D_{d,d}$ may be constructed using modified nodal analysis [9] and a canonical transformation (for a step-by-step guide, see [10]). Alternatively, there exist a number of tools that can perform these steps automatically, e.g. the Simscape package in MATLAB [11, p. 3-54].

The equations are eliminated to yield a relationship established between the external input voltage and the "closed-loop" damper terminal voltage,

$$T_{cl}(s) \triangleq [1 - T_{d,d}(s)Y(s)]^{-1}T_{d,in}(s), \tag{11}$$
$$v_{out}(s) = T_{cl}(s)v_{in}(s). \tag{12}$$

Likewise, the relationship between the external input voltage and the "closed-loop" damper terminal current is,

$$i_d(s) = [Y(s)T_{cl}(s)]v_{in}(s). \tag{13}$$

B. Resonant voltage limit via $\mathcal{H}_\infty$ norm

The $\mathcal{H}_\infty$-norm of a general transfer function $T(s)$ is defined

$$\|T(s)\|_\infty \triangleq \max_{\mathrm{Res}>0} \sigma_{max}[T(s)], \tag{14}$$

where $\sigma_{max}(\cdot)$ computes the maximum singular value of a matrix argument.

As in the case of a stable single-input, single-output transfer function, $T_{cl}(s)$, defined in (11) to be the voltage gain of the damper, the $\mathcal{H}_\infty$-norm *coincides* with the maximum gain,

$$\|T_{cl}(s)\|_\infty \equiv \max_{\omega\in\mathbb{R}} |T_{cl}(j\omega)|, \tag{15}$$

which is the design constraint as described in (2).

C. Dissipation via $\mathcal{H}_2$ norm

In Section II-B, the worst-case dissipation is defined as the solution to the optimization problem (5). In this subsection, we show that the optimization may be solved using exactly three $\mathcal{H}_2$ norm evaluations.

To begin, we note that by Parseval's theorem, the Fourier transform of $v^\star_{in}(t)$ in (3) must also be the solution to the maximization

$$\hat{v}^\star_{in}(j\omega) = \begin{array}{ll} \text{maximize} & \mathrm{Re}\int_{-\infty}^{\infty} \hat{v}_d(j\omega)\overline{\hat{i}_d(j\omega)}\,\mathrm{d}\omega, \\ \text{subject to} & |\hat{v}_{in}(j\omega)| \le \left|\dfrac{\omega_{sw}}{j\omega + \omega_{sw}}\right|, \end{array} \tag{16}$$

in which we have substituted the definition of $\mathcal{BV}(\omega_{sw})$ in (5).

In a linear system, all the frequencies are decoupled, and the objective in (16) is maximized by individually maximizing $\hat{v}_d$ each frequency. Hence, the value of P_{max} is given in closed-form

$$P_{max} = \mathrm{Re}\int_{-\infty}^{\infty} \hat{v}_d(j\omega)\overline{\hat{i}_d(j\omega)}\,\mathrm{d}\omega, \quad \text{subject to } \hat{v}_{in}(j\omega) = \frac{\omega_{sw}}{j\omega + \omega_{sw}}. \tag{17}$$

To evaluate the expression, we introduce the $\mathcal{H}_2$-norm, which is defined for a general transfer function $T(s)$ as

$$\|T(s)\|_2 \triangleq \sqrt{\frac{1}{2\pi}\int_{-\infty}^{\infty} \mathrm{tr}[T(j\omega)^* T(j\omega)]d\omega},$$

where $\mathrm{tr}(\cdot)$ is takes the trace (i.e. sum of the diagonal elements) of a matrix argument. Immediately, (17) can be

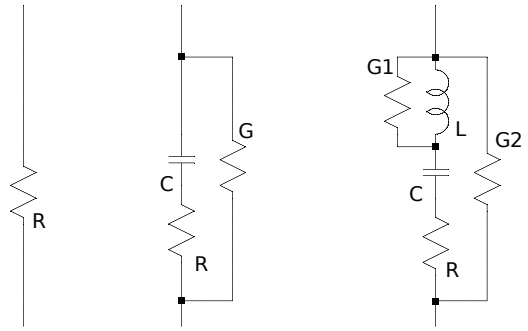

(a) (b) (c)

Figure 3: Passive transfer function realizations: (a) zeroth order; (b) first order; (c) second order.

written in terms of three $\mathcal{H}_2$ norm evaluations,

$$\begin{aligned}\frac{1}{\pi}P_{max} =& \frac{1}{\pi}\int_{-\infty}^{\infty} \mathrm{Re}\{\hat{v}_d(j\omega)\overline{\hat{i}_d(j\omega)}\}\, d\omega \\ =& \frac{1}{2\pi}\int_{-\infty}^{\infty} |\hat{v}_d + \hat{i}_d|^2 - |\hat{v}_d|^2 - |\hat{i}_d|^2\, d\omega \\ =& \|\hat{v}_d(s) + \hat{i}_d(s)\|_2^2 - \|\hat{v}_d(s)\|_2^2 - \|\hat{i}_d(s)\|_2^2,\end{aligned}$$

by noting that for any complex x, y, we have $2\mathrm{Re}\{x\overline{y}\} = |x+y|^2 - |x|^2 - |y|^2$.

In turn, each $\mathcal{H}_2$ norm term may be evaluated in terms of $Y(s)$, $T_{cl}(s)$ and the input spectrum $\hat{v}_{in}^{\star}(s)$, as in

$$\hat{v}_d(s) = T_{cl}(s)\hat{v}_{in}^{\star}(s), \tag{18}$$

$$\hat{i}_d(s) = Y(s)T_{cl}(s)\hat{v}_{in}^{\star}(s). \tag{19}$$

D. Circuit realizability

In order to impose that the transfer function, $Y(s)$, should be realizable as the terminal admittance of a linear passive circuit, a necessary and sufficient condition for a transfer function is the passivity property.

Definition 2. The transfer function $Y : \mathbb{C} \to \mathbb{C}$ is said to be passive if it is stable, and satisfies

$$Y(\overline{s}) = \overline{Y(s)} \qquad \forall s \in \mathbb{C}, \tag{20}$$

$$Y(s) + \overline{Y(s)} \geq 0 \qquad \forall \mathrm{Re}\{s\} > 0. \tag{21}$$

In turn, for the damper design problem, one can show that every passive, proper transfer function of zeroth, first and second order can be realized as the terminal admittance of the three topologies shown in Fig. 3. Once a solution $Y(s)$ has been computed, the circuit component values may be obtained by fitting the poles and zeros to one of these three topologies.

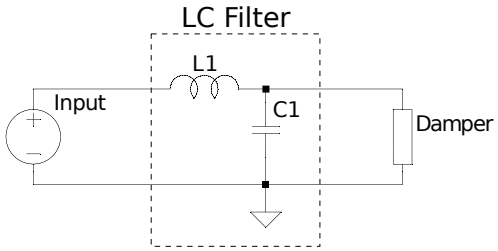

Figure 4: LC Filter damper design

E. Nonsmooth, nonconvex optimization

Combined, the damper design problem (1) is reformulated into the following mixed $\mathcal{H}_2/\mathcal{H}_\infty$ controller synthesis problem

$$\begin{aligned}\underset{A_Y,B_Y,C_Y,D_Y}{\text{minimize}} \quad & \|\hat{v}_d(s) + \hat{i}_d(s)\|_2^2 - \|\hat{v}_d(s)\|_2^2 - \|\hat{i}_d(s)\|_2^2 \\ \text{subject to} \quad & \text{(8)-(11), (18), (19),} \\ & \|T_{cl}(s)\|_\infty \leq \text{specs}, \\ & Y(s) \text{ is passive.}\end{aligned}$$

Optimization problems similar to the above are ubiquitous in control theory. The standard, efficient approach for a conservative global solution is to formulate a suitable convex linear matrix inequality (LMI), by linearizing the concave part of the objective [12], substituting the Kalman-Yakubovich-Popov Lemma, and adopting a suitable change of variables [13], [14]. Unfortunately, a key step in LMI methods assumes that the controller, $Y(s)$, is of the same order as the plant, $T_{d,in}(s)$ and $T_{d,d}(s)$. This is highly undesirable for our problem, because high order dampers are difficult and impractical to realize.

Instead, global optimality is sacrificed in this paper, and the design problem is solved using classic algorithms for (local) nonlinear optimization, such as interior-point [15] and sequential quadratic programming [16]. These methods work surprisingly well because the objective and constraints are smooth *almost everywhere* [17], [18], [19]. In turn, there is considerable experience in the controls community that the local solution is very often also the global solution [20], [21], [22].

In our implementation, the $\mathcal{H}_\infty$, $\mathcal{H}_2$ norms, the passivity constraint and their gradients are evaluated using the steps in [3], and the resulting constrained optimization is locally solved using the `interior-point` algorithm of the `fmincon` function in the MATLAB optimization toolbox, which is based on [15].

IV. Design Example 1: Trade-off frontier for high-order Damping

Traditional dampers and snubbers are constructed from just two components: a resistor in series with a capacitor. Their design procedure is simple: the resistor is sized to provide sufficient damping for a designated resonant frequency, and the capacitor is sized so that the combined branch appears like an open circuit over the frequencies below it, thereby minimizing

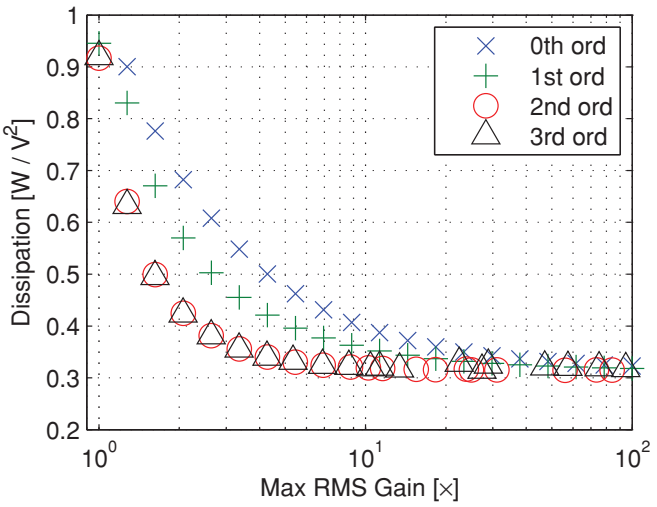

Figure 5: Pareto frontier for LC damper design input spectrum $\omega_{knee} = 1/3$ rad/s;

losses [23], [24]. Indeed, this simplicity is a significant reason for their widespread practical use.

However, more complicated damper designs are also possible, and under suitable conditions, these can achieve a better overall trade-off between damping and dissipation. For example, [25] describes a damper design in which the lead inductance of the damper is explicitly considered as a part of the damper, to yield a second-order inductor-resistor-capacitor topology. The authors found that a considerably more selective resonance suppression could be achieved, as compared to the simpler resistor-capacitor damper.

A. Limits of performance

In order to meaningfully compare dampers of different orders, the limits of performance must be quantified in a rigorous manner. A powerful analytical tool is the *Pareto frontier*: the set of damper designs for which the dissipation cannot be decreased further without worsening the frequency response, and conversely, the frequency response cannot be improved further without increasing dissipation. If a Pareto frontier is constructed for each fixed-order, then a decision to increase the damper order may be justified by a sufficiently large shift in the corresponding frontier.

In fact, the Pareto frontier may be explicitly computed using the approach in this paper. This is so because a globally optimal design to the specifications in Section II is Pareto optimal by definition, being the least-dissipative damper that still achieves a particular maximum frequency response. In turn, locally optimal designs can be efficiently computed using the optimization in Section III, and used to approximate the frontier.

The computational approach to Pareto optimality is illustrated with a simple, intuitive example. Consider the simple LC filter, shown in Fig. 4, which is ubiquitous in power electronics. To simplify circuit analysis, we set $L = C = 1$ to yield a resonant frequency of $\omega_0 = 1$. In turn, the input spectrum is assumed to have a switching frequency of $\omega_{sw} = 1/3$, i.e. one third of the resonant frequency of the filter.

Figure 5 plots the approximate Pareto frontier for dampers of differing orders, as computed using the optimization in Section III, showing several interesting phenomena:

1) There exists a fundamental lower-bound to the dissipation experienced of approximately 0.33 $\mathrm{W/V^2}$, which is common to dampers of all orders.
2) The third-order damper performs no better than the second-order damper.
3) For lower values of RMS gain, e.g. less than $10\times$, the reduction in dissipation available by increasing the damper order is considerable. For instance, the dissipation of the zeroth-order snubber at $3\times$ gain is approximately 0.55 $\mathrm{W/V^2}$, which is the same as that for the first-order snubber at $2\times$ gain and the second-order snubber at $1.5\times$ gain.
4) For higher values of RMS gain, e.g. greater than $10\times$, all damper orders experience about the same amount of dissipation. Increasing the damper order is less justifiable.

With these points in mind, the Pareto optimal second-order damper appears to be an attractive option when the RMS gain is limited to practical values of around $1.5\times$ to $2\times$. Within this range, the reduction in dissipation is between 20-30 %, which is large enough to allow smaller circuit components to be used and stand-by power consumption to be reduced.

B. Closed-loop characteristics

As a sanity check to verify the results above, it is helpful to examine the actual dampers synthesized by the optimization. Figure 6 shows the Bode plot for the lowest-dissipation zeroth, first, second, and third order damper for a maximum frequency response of up to $1.5\times$. As shown, all four dampers minimize their admittances away from resonance, while attempting to appear as a resistor of ~0.7 conductance at resonance. This exact value can be explained by noting that when a LC filter is undamped, the maximum frequency response is approximately equal to the quality factor Q. In turn, the conductance to achieve a quality factor of 1.5 for a resonator with $L = C = 1$ is 0.667. The discrepancy arises because the resonant frequency has been shifted slightly by the damping.

Finally, the frequency response of the damped LC filters are shown in Fig. 7a, showing that the maximum response objective of $T_{max} \leq 1.5$ has indeed been satisfied. We expect the peak step-response of each damped filter to also be similar, but not necessarily equal to 1.5. This is confirmed in Fig. 7b. Interestingly, while the second- and third-order dampers are less dissipative than the zeroth- and first-order dampers, their instantaneous peak during a step response is actually slightly worse.

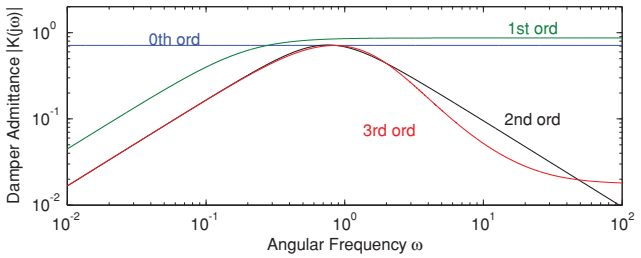

(a)

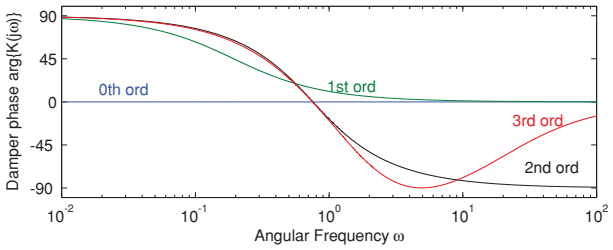

(b)

Figure 6: Controller $Y(s)$ (a) magnitude and (b) phase, for optimal designs at $T_{max} = 1.5$. All four designs attempt to have the snubber appear resistive (i.e. with zero phase) at the resonant frequency with approximately the same admittance.

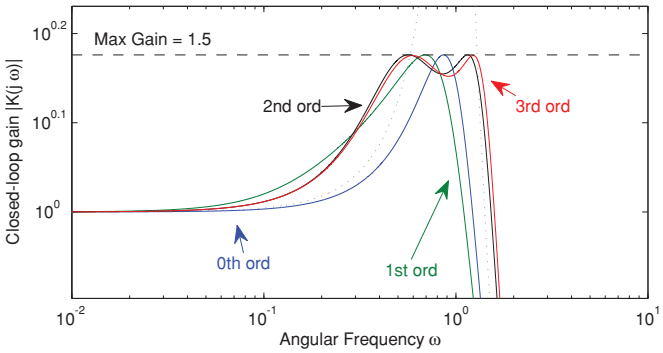

(a)

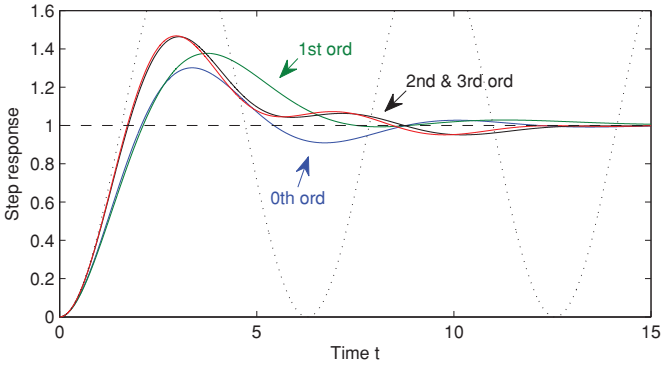

(b)

Figure 7: Optimal closed-loop performance: (a) frequency response; (b) step response.

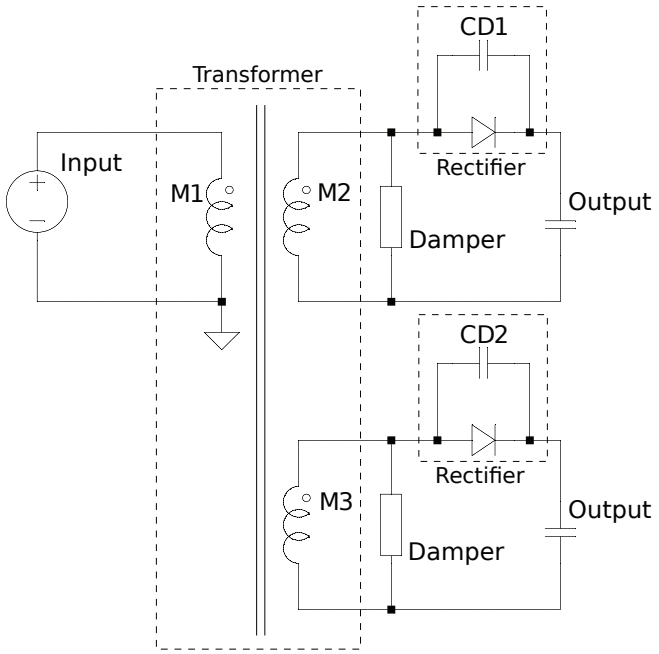

Figure 8: Idealized representation of an isolated, multiple output DC-DC converter with two output terminals.

V. Design Example 2: Coupled Resonances in High-Order Plant

A different but complementary setting in which damper design is difficult is when resonances are coupled. To give a practical example, consider the isolated, multiple output converter shown in Fig. 8. It is common for the parasitic diode capacitances to resonate, and dampers are often added at the transformer secondaries, both to avoid excessive electromagnetic interference, as well as to protect the rectifier from overvoltage. The damper design problem is surprisingly difficult, because all of the resonances are coupled over all of the components in the circuit.

As before, the analytical difficulties are alleviated by the use of an optimization approach. But important for this case is the fact that it allows the dampers to be simultaneously designed, all while respecting and addressing the presence of coupled resonances. As we show in Section V-B, this allows designs to be less conservative than if each damper were considered individually.

A. Model description

To highlight the challenges of coupled resonances, we examine a particularly difficult example: a transformer with ten outputs, all at different turns ratios, resonating with ten independent parasitic capacitors. For this, the transformer is modeled as coupled inductors, with primary self-inductance of 1, ideal turns ratios to the secondaries varying linearly from 1 to 2, and coupling coefficients of $\kappa = 0.9$. The output capacitors are modeled as electrical shorts (an assumption that is valid at the frequencies of interest), and each parasitic capacitor is normalized to have a capacitance of 1. The input

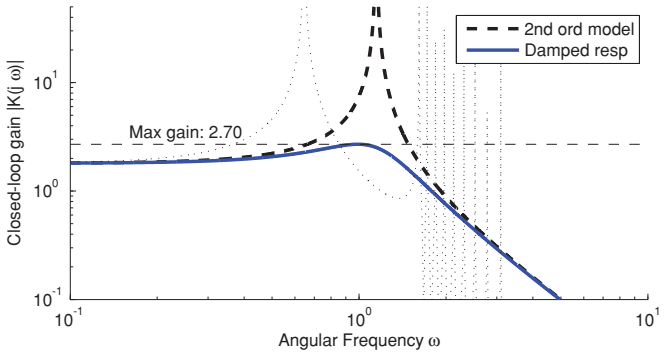

Figure 9: Independent damping of coupled resonance. A fictitious second-order model is constructed for a given output phase, and the damper is designed to meet an $\mathcal{H}_\infty$ norm specification for this model. The actual undamped response is shown in dots.

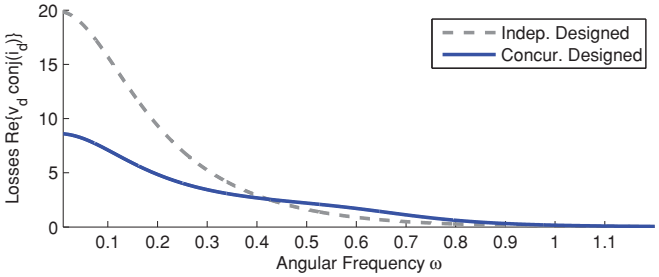

Figure 10: Comparison of frequency-dependent dissipation for an input spectrum with $\omega_{sw} = 0.2$.

spectrum, previously described in Section II-B, is assumed to have a corner frequency corner of $\omega_{sw} = 0.2$ rad/sec.

The resonant peaking constraint for the optimization is for each *normalized* $\mathcal{H}_\infty$ norm to be at most 1.5. To expand on this description with an example, consider the secondary with an ideal turns ratio of 2. The effective turns ratio for this secondary is κ times the ideal, i.e. $2 \times 0.9 = 1.8$, and all frequencies in the passband are amplified by this value. In this case, our design constraint is to limit resonant peaking to be at most 1.5 times this value, i.e. $1.8 \times 1.5 = 2.7$. Our objective is to design the damper such that the *regular* $\mathcal{H}_\infty$ norm is at most 2.7.

B. Independent vs concurrent design

Despite the coupling between transformer secondaries, it is indeed possible to design each damper port-by-port. Considering each port (i.e. transformer secondary) on its own, a common ad-hoc assumption is to take all other ports as open circuits. This eliminates all but a single transformer leakage inductance and its corresponding parasitic capacitor, and yields a fictitious second-order model for the transformer secondary, which can then be used to design a suitable damper, as shown in Fig. 9. However, the fictitious model is not necessarily a good representation for the underlying system. In this case, its resonant frequency does not actually correspond to any of the resonant frequencies of the "real" model.

Table I: Independent and concurrent design of resistor dampers, to limit *normalized* $\mathcal{H}_\infty$ to be at most 1.5 (see text for details).

	Independent			**Concurrent**		
	R	$\mathcal{H}_\infty$	Diss.	R	$\mathcal{H}_\infty$	Diss.
Out 1	0.611	1.00	0.614	9.791	1.342	0.053
Out 2	0.679	1.00	0.684	8.864	1.348	0.073
Out 3	0.747	1.00	0.754	12.219	1.367	0.065
Out 4	0.814	1.00	0.825	14.307	1.377	0.067
Out 5	0.882	1.00	0.897	7.582	1.393	0.148
Out 6	0.950	1.00	0.970	13.838	1.412	0.095
Out 7	1.018	1.00	1.044	16.271	1.432	0.094
Out 8	1.086	1.00	1.118	14.033	1.455	0.126
Out 9	1.154	1.00	1.194	1.051	1.440	1.867
Out 10	1.222	1.00	1.271	0.677	1.391	3.158
Total			9.371			5.748

More importantly, the assumption also produces overly conservative designs, particularly when many ports are considered. Each damper had been separately designed to dissipate energy for the entire transformer. So when the dampers are combined for the coupled system, more damping is introduced than necessary, resulting in more dissipation.

The above point is illustrated in Table I. To keep the example simple and intuitive, we restrict ourselves to designing zeroth order dampers, i.e. simple resistors. In the "Independent" column, each resistor was individually designed to meet a normalized $\mathcal{H}_\infty$ norm of 1.5 across its own secondary, while in the "Concurrent" column, all resistors are designed simultaneously to meet a normalized $\mathcal{H}_\infty$ norm constraint of 1.5 across all secondaries. As shown, the independently designed dampers vastly overshoot the design objective when combined for the coupled system, overdamping every secondary to the minimum normalized $\mathcal{H}_\infty$ norm of 1. By contrast, the concurrent design maintains a normalized $\mathcal{H}_\infty$ norm between 1.35 and 1.46 over each secondary. Accordingly, as shown in Fig. 10, the independently-designed dampers dissipate around 63% more power than the concurrent design.

C. Closed-loop Performance

The frequency responses from the input voltage to the voltages at each of the outputs is shown in Fig. 11; note that the low frequency gain for each winding differs by the turns ratio. Both design methods achieve the desired resonant peak constraint, but the independently-designed dampers produce a grossly overdamped response and higher power dissipation. This overdamping is also readily apparent in the step responses of each of the outputs shown in Fig. 12a; in comparison, the concurrently designed dampers in Fig. 12b show some overshoot and ringing, but well within specification.

VI. Conclusions

The linear damper design problem of balancing frequency response and energy dissipation has been shown to admit an *exact* control synthesis formulation, which can be solved using standard algorithms for nonsmooth, nonconvex optimization.

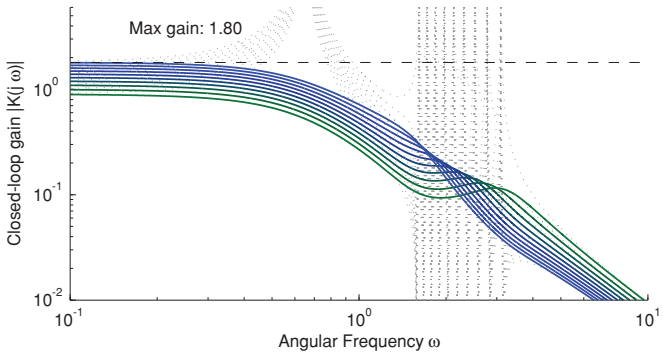

(a)

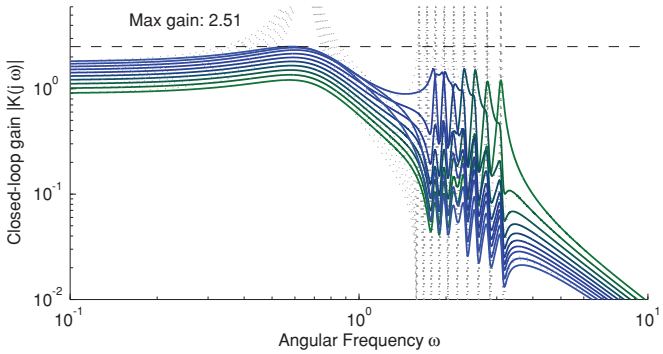

(b)

Figure 11: Frequency response comparison of the (a) independently designed damper against the (b) concurrently designed damper. The undamped response is shown in dots.

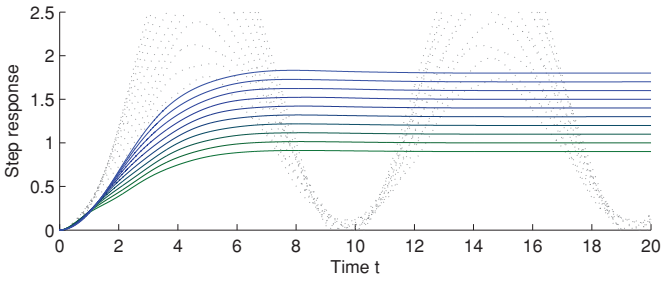

(a)

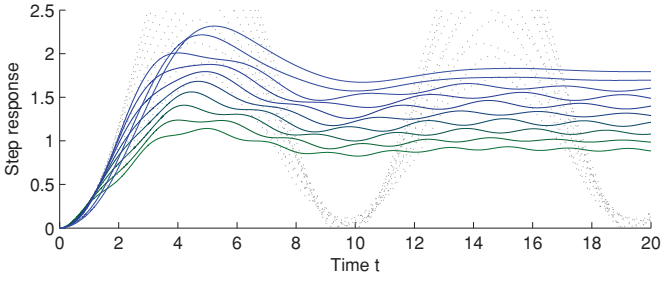

(b)

Figure 12: Step response comparison of the (a) independently designed damper against the (b) concurrently designed damper. The undamped response is shown in dots.

The computational approach allows high-order dampers to be designed and their performance limits to be quantified. In the same manner, it also allows high-order plants with coupled resonances to be damped, without making overtly conservative assumptions.

Our work has assumed that models for resonant circuits are known exactly, so that dampers may be carefully tuned to maximize performance. But in situations where model parameters are uncertain (e.g. due to measurement error) or time-varying (e.g. due to temperature dependence), the approach may no longer be valid. Hence, an important future work is to extend the control synthesis formulation to account for the issue of *robustness*.

VII. Acknowledgments

The authors are grateful for the financial support of this work provided by the MIT Energy Initiative, the Grainger Foundation, and the Skolkovo-MIT Initiative in Computational Mathematics.

References

[1] K. Zhou, J. C. Doyle, K. Glover *et al.*, *Robust and optimal control*. Prentice hall New Jersey, 1996, vol. 40.

[2] F. Costa, C. Gautier, E. Laboure, and B. Revol, *Electromagnetic Compatibility in Power Electronics*. John Wiley & Sons, 2014.

[3] S. P. Boyd and C. H. Barratt, *Linear controller design: limits of performance*. Prentice Hall Englewood Cliffs, NJ, 1991.

[4] J. Rodriguez, J.-S. Lai, and F. Z. Peng, "Multilevel inverters: a survey of topologies, controls, and applications," *Industrial Electronics, IEEE Transactions on*, vol. 49, no. 4, pp. 724–738, 2002.

[5] D. G. Holmes and T. A. Lipo, *Pulse width modulation for power converters: principles and practice*. John Wiley & Sons, 2003, vol. 18.

[6] F. Z. Peng, J.-S. Lai, J. W. McKeever, and J. VanCoevering, "A multilevel voltage-source inverter with separate DC sources for static var generation," *Industry Applications, IEEE Transactions on*, vol. 32, no. 5, pp. 1130–1138, 1996.

[7] M. K. Kazimierczuk and D. Czarkowski, *Resonant power converters*. John Wiley & Sons, 2012.

[8] Y. Katznelson, *An introduction to harmonic analysis*. Cambridge University Press, 2004.

[9] C.-W. Ho, A. E. Ruehli, and P. A. Brennan, "The modified nodal approach to network analysis," *Circuits and Systems, IEEE Transactions on*, vol. 22, no. 6, pp. 504–509, 1975.

[10] M. Gerdin, "Computation of a canonical form for linear differential-algebraic equations," 2004.

[11] *Simscape User's Guide*, The Mathworks, Inc.

[12] R. Horst and P. M. Pardalos, *Handbook of global optimization*. Springer Science & Business Media, 2013, vol. 2.

[13] M. Chilali and P. Gahinet, "$\mathcal{H}_\infty$ design with pole placement constraints: an LMI approach," *Automatic Control, IEEE Transactions on*, vol. 41, no. 3, pp. 358–367, 1996.

[14] C. Scherer, P. Gahinet, and M. Chilali, "Multiobjective output-feedback control via LMI optimization," *Automatic Control, IEEE Transactions on*, vol. 42, no. 7, pp. 896–911, 1997.

[15] R. H. Byrd, M. E. Hribar, and J. Nocedal, "An interior point algorithm for large-scale nonlinear programming," *SIAM Journal on Optimization*, vol. 9, no. 4, pp. 877–900, 1999.

[16] P. T. Boggs and J. W. Tolle, "Sequential quadratic programming," *Acta numerica*, vol. 4, pp. 1–51, 1995.

[17] J. V. Burke, A. S. Lewis, and M. L. Overton, "A robust gradient sampling algorithm for nonsmooth, nonconvex optimization," *SIAM Journal on Optimization*, vol. 15, no. 3, pp. 751–779, 2005.

[18] J. V. Burke, D. Henrion, A. S. Lewis, and M. L. Overton, "Stabilization via nonsmooth, nonconvex optimization," *Automatic Control, IEEE Transactions on*, vol. 51, no. 11, pp. 1760–1769, 2006.

[19] A. S. Lewis and M. L. Overton, "Nonsmooth optimization via quasi-newton methods," *Mathematical Programming*, vol. 141, no. 1-2, pp. 135–163, 2013.

[20] P. Apkarian and D. Noll, "Nonsmooth $\mathcal{H}_\infty$ synthesis," *Automatic Control, IEEE Transactions on*, vol. 51, no. 1, pp. 71–86, Jan 2006.
[21] J. Burke, D. Henrion, A. Lewis, and M. Overton, "HIFOO-a MATLAB package for fixed-order controller design and $\mathcal{H}_\infty$ optimization," in *Fifth IFAC Symposium on Robust Control Design, Toulouse*, 2006.
[22] P. Gahinet and P. Apkarian, "Structured $\mathcal{H}_\infty$ synthesis in MATLAB," *Proc. IFAC, Milan, Italy*, 2011.
[23] W. McMurray, "Optimum snubbers for power semiconductors," vol. IA-8, no. 5, pp. 593–600, 1972. [Online]. Available: http://ieeexplore.ieee.org/stamp/stamp.jsp?arnumber=4158300
[24] ——, "Selection of snubbers and clamps to optimize the design of transistor switching converters," in *Power Electronics Specialists Conference, 1979 IEEE*. IEEE, 1979, pp. 62–74.
[25] T. Yamaguchi, K. Kurita, and T. Sudo, "On-board snubber circuit for damping of anti-resonance peak in total PDN," in *CPMT Symposium Japan (ICSJ), 2014 IEEE*, 2014, pp. 91–94. [Online]. Available: http://ieeexplore.ieee.org/stamp/stamp.jsp?arnumber=7009617